# Determination of the $\alpha$-decay half-life of $^{210}$Po based on film and slice bismuth samples at room temperature

Q. Z. Zhao,[1] X. M. Wang,[1] W. Wang,[2] M. He,[1] K. J. Dong,[1] C. J. Xiao,[1] X. D. Ruan,[3] H. T. Shen,[4] S. Y. Wu,[1] X. R. Yang,[1] L. Dou,[1] Y. N. Xu,[1] L. Cai,[3] F. F. Pang,[4] H. Zhang,[5] Y. J. Pang,[4] and S. Jiang[1,*]

[1]*China Institute of Atomic Energy, Beijing 102413, People's Republic of China*

[2]*China National Nuclear Corporation, Beijing 100822, People's Republic of China*

[3]*College of Physical Science and Technology, Guangxi University, Nanning 530004, People's Republic of China*

[4]*College of Physical Science and Technology, Guangxi Normal University, Guilin 541004, People's Republic of China*

[5]*Technical Physics Institute of Heilongjiang Academy of Sciences, Harbin 150086, People's Republic of China*

(Received 10 July 2015; revised manuscript received 27 September 2015; published 20 November 2015)

The $\alpha$ decay rate of $^{210}$Po was measured in a film sample ($^{210}$Po @$Bi_2O_3$) and a slice sample ($^{210}$Po @Bi metal), respectively. The former was used as a reference sample. The half-lives of $^{210}$Po @$Bi_2O_3$ and $^{210}$Po @Bi metal environments were observed to be ($138.40 \pm 0.21$ d) and ($138.87 \pm 0.87$ d) at room temperature, respectively. It was found that the half-life of $^{210}$Po is consistent with international recommendations within the uncertainty limits, and we did not find any deviation of the $\alpha$ decay rate of $^{210}$Po between film sample ($^{210}$Po @$Bi_2O_3$) and slice sample ($^{210}$Po @Bi metal).

DOI: 10.1103/PhysRevC.92.054616 PACS number(s): 23.60.+e, 21.10.Tg, 27.80.+w

## I. INTRODUCTION

It is generally believed that the values of $\alpha$ half-lives are constant and independent of the external environment of radioactive nuclei. However, recently, the study of the half-lives of radionuclides depending on the external environment of the decaying nucleus has become a hot research topic [1–17], since different experiments showed varying results concerning this controversial question. Nuclear waste and its reprocessing is rapidly becoming a global environmental problem, and if the decay rates of radioactive waste products can be increased by changing the surrounding material, it would be a major breakthrough in the disposal of accumulating radioactive waste [18]. Therefore, we designed an experiment to study the effect of electron density of the material surrounding the decaying nucleus on the $\alpha$ half-life of $^{210}$Po, which we describe here.

It is known that the presence or absence of atomic electrons can affect the probability of electron capture decay [19–21]. $^{209}$Bi provided external electron density because of its crystal rhombohedral structure to investigate the possible effects on $\alpha$ decay half-lives of $^{210}$Po. The $^{210}$Po nucleus decays directly to the $0^+$ ground state of $^{206}$Pb with a 100% branching ratio. The $\alpha$ decay rate may depend on the density of the quasifree electron cloud surrounding the nuclei decaying in metallic environment [14,15,22], which is the focus of our study. In this article, we investigate if the $\alpha$ decay rates of $^{210}$Po can be intentionally increased by embedding in particular metals. It has been claimed that half-lives of radioactive nuclei embedded in metals would be significantly affected by the electron screening provided by the metal. However theoretical calculations [23] showed that the influence of the metal environment on decay constants of radionuclides is very small.

There are many experiments testing this effect. For example, a study showed that the number of $\alpha$ particles from $^{221}$Fr were reduced by 0.30 (17)% and 0.42 (21)% when placed in the metals gold or tungsten, respectively, compared to when placed in the semiconductor silicon [12]. However, Su [5] reported an independent measurement of $\alpha$ particle half-life of $^{147}$Sm in a metallic environment at room temperature. The results showed that the $\alpha$ half-life of $^{147}$Sm is consistent with the recommended value within the uncertainty range.

A rough estimate of the free electron density of $^{209}$Bi was found to be $10^{28}$ m$^{-3}$ using standard solid state physics. Because of the unique rhombohedral crystal structure of $^{209}$Bi, the pure $\alpha$-emitter $^{210}$Po (decay energy $E = 5.30$ MeV) may be significantly affected by such an electron density. Therefore, it is interesting to investigate the question: "How does the $\alpha$ decay rate of $^{210}$Po change when embedded inside the rhombohedral crystal structure of $^{209}$Bi?" Here, the half-life of $^{210}$Po in the $^{209}$Bi metal crystal structure was compared with that in $Bi_2O_3$ as a reference. An estimate of the value of free electrons in $Bi_2O_3$ is approximately $10^{19}$ m$^{-3}$ using eigenvalues in standard solid state physics. Thus, the different chemical forms of Bi metals may have different screening potentials from the distribution of quasifree electrons. To address this question, we experimentally investigated the $\alpha$ half-life by placing it in these two materials with substantially different electron distributions.

Ohtsuki *et al.* [1] found that the half-life of $^{7}$Be in $C_{60}$ is shorter than when it is in natural Be. They attributed this result to the special dynamic condition of the electrons inside the $C_{60}$ cage. The method used by Ohtsuki to implant $^{7}$Be in $C_{60}$ cages was ion implantation. We do not use that method in this experiment because the distribution of implanted ions may not be homogeneous and the implantation depth will be near the surface layers, minimizing any contribution from the electron distribution of the host material. To avoid these sources of systematic error, in the present experiment, the $^{210}$Po nuclei were distributed homogeneously in the samples instead by

*jiangs@ciae.ac.cn

 

neutron activation of $^{209}$Bi. In this article, we report the details of the experimental setup for the decay measurement and the results of our analysis.

## II. EXPERIMENT

### A. Experiment design

In order to investigate the possible effects of external electron distributions on the $\alpha$ decay probability of $^{210}$Po, we performed a measurement of its half-life in both a $^{209}$Bi rhombohedral metallic crystal structure ($^{210}$Po @Bi metal) and in a chemical film sample ($^{210}$Po @$Bi_2O_3$). The $^{210}$Po radioactivity was produced in both samples by neutron irradiation via the $^{209}$Bi$(n,\gamma)^{210}$Bi reaction. We carefully controlled possible sources of systematic error in the following ways:

(1) The $\alpha$ radioactivities in both samples were measured in the same spectrometer chamber with an identical setup, to avoid any effects from geometry, detector efficiency, and background sources. The detector dead-time was never greater than 0.5% during the measurements.

(2) The half-life measurements were carried out for at least 350 days, or nearly three nominal half-lives of $^{210}$Po (138.3763(17) d [24,25]), in order to minimize any minor variation in the instantaneous decay probability to the overall deduced half-lives.

(3) In order to obtain a high signal-to-noise ratio and sufficient statistics, we used the maximum thermal neutron flux during the sample activation via $^{209}$Bi$(n,\gamma)^{210}$Bi.

(4) Because the surface layers of the pure $^{209}$Bi metallic target could oxidize under ambient laboratory conditions (leading to a similar chemical structure to the film sample), the metallic target was manufactured and stored in a high vacuum environment (the vacuum pressure is estimated to be $10^{-4}$ Pa).

(5) We annealed only the metallic sample after neutron irradiation to repair any damage to the lattice structure. Thus, by the sample preparation methods, we could ensure a significant difference of the quasifree electron density between the two samples.

(6) To achieve high accuracy and precision of the timing measurements, the timing measurements were synchronized to the standard clock time provided by the National Time Service Center of the Chinese Academy of Sciences.

### B. Sample preparation

The high purity $^{209}$Bi(6N) powder was used to prepare samples, purchased commercially from Alfa Aesar Company. For the film sample, 60 mg cm$^{-2}$ of bismuth was evaporated over an area of 10.0 mm in diameter on a high purity copper substrate. This was done layer by layer, first under vacuum and then while being oxidized during the evaporating process. With the above production method, a lattice structure is produced with a given quasifree electron distribution in the film.

The metallic $^{209}$Bi sample was produced by vacuum melting and vacuum evaporation of 2.0 mm also over an area 10.0 mm in diameter for consistency between the two samples. The vacuum evaporation system for the metallic sample included a vacuum annealing furnace to produce the lattice crystalline structure in $^{209}$Bi. Finally, a thin aluminium foil (3 nm) was placed over the bismuth sample, again under vacuum, to avoid any surface oxidation of the bismuth and ensure a structural difference between the film sample and the metallic sample.

### C. Sample irradiation

Care is required in the sample irradiation procedure to ensure the samples retained their distinct structure, as the melting point (271.4 °C) of bismuth is quite low, and an oxide layer may easily form, even under vacuum conditions. To control these possible issues, the samples were first placed in a narrow quartz glass tube (diameter 12 mm). Prior to storing the samples in the quartz tube, the tube was evacuated with a turbo molecular pump to remove any contaminants. After placing the samples in the quartz tube, we sealed the quartz tube by heating; during this sealing process, the quartz tube was cooled with liquid nitrogen to ensure the samples were not heated by the sealing process. Finally, the prepared samples housed in the quartz tube were placed in an aluminium can, which was irradiated at the H4 channel of the swimming pool reactor of the China Institute of Atomic Energy (CIAE), where the local neutron flux is $10^{13}$ s$^{-1}$ cm$^{-2}$ as determined by a Zr detection sheet over the course of 24 h.

$^{209}$Bi nuclei were transformed into the $^{210}$Po radionuclide via the $^{209}$Bi$(n,\gamma)^{210}$Bi$(\beta^-)^{210}$Po sequence induced by thermal neutrons followed by a 5.01 d $\beta$-decay half-life. With this activation method, the $^{210}$Po nuclei are homogeneously distributed in the samples, as the thermal neutron mean free path is much larger than the sample size. The resulting fraction of $^{210}$Po / $^{209}$Bi was estimated to be $10^{-8}$. Following the neutron activation, the metallic sample only was baked in a vacuum electric oven for 1 h at 130 °C to repair any lattice damage caused during the radiation exposure.

### D. Measuring equipment

It is possible that the neutron activation might produce some background $\alpha$-emitting species in addition to $^{210}$Po. To check such a source of error, the samples were monitored with a high-purity germanium (HPGe) detector for 2 h each. This is a standard technique to analyze the resulting radioactivity of neutron-irradiated samples, since $\alpha$-delayed $\gamma$-decay allows for the unique identification of the parent nucleus. However, no other radioactivities were observed in the $\gamma$-ray spectra, and we conclude that the $\alpha$ activity of the two samples can be entirely attributed to the decay of $^{210}$Po.

We measured the residual energy of the $\alpha$ particles emitted from the samples with silicon surface barrier detectors (SBD) with an area of 1200 mm$^2$ produced by ORTEC. The silicon detectors have nearly 100% efficiency and high energy resolution, and were absolutely calibrated with a $^{239}$Pu - $^{241}$Am standard source. The samples and detectors were placed in a vacuum chamber manufactured by ORTEC, equipped with a special high-performance O-ring set into the casted chamber surface creating an excellent seal. The same setup was used for the measurement of the alpha spectra from both the metallic

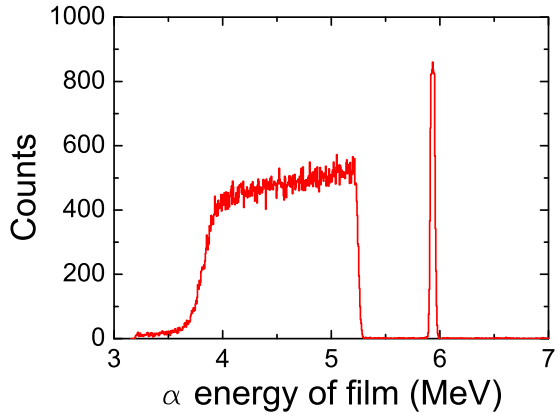


FIG. 1. (Color online) $\alpha$ spectra of the film sample. The $\alpha$ energy of $^{210}$Po on the surface of the sample is about 5.3 MeV. The sharp peak on the right side is from a research pulser.

and the film samples. Each sample was housed in a suitable depression in a polytetrafluoroethylene tray in the chamber 35 mm from the SBDs, which is carefully fixed in the chamber to ensure the silicon detector solid angle is constant between the measurements of the two samples.

The $\alpha$ spectra measured by the SBDs were analysed with the ORTEC Spectrum Master to calculate the half-lives. Furthermore, we checked the $\alpha$-background in the chamber for 5 h before each measurement of each sample and for 5 h after each measurement of each sample, but no such $\alpha$ particles were observed.

## III. DATA ANALYSIS AND RESULTS

We could observe nearly the full energy for $\alpha$ particles emitted from the film sample as shown in Fig. 1, but owing to the energy loss of $\alpha$ particles in the thick metallic sample, we could only measure their residual energies which had a long tail towards lower energy as shown in Fig. 2. We analyzed the $\alpha$ spectra over the energy range of 3.00 to 5.30 MeV. Independent analyses were performed for the different types

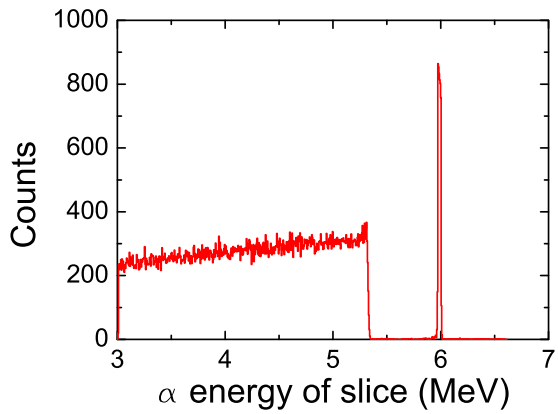


FIG. 2. (Color online) $\alpha$ spectra of the slice sample. The maximum $\alpha$ energy of $^{210}$Po in the slice target sample is 5.3 MeV. The sharp peak on the right side is from a research pulser.

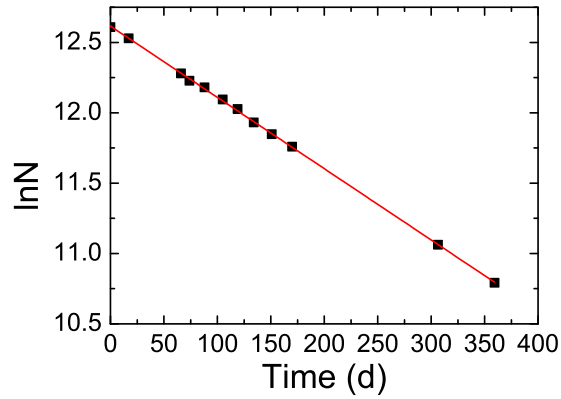


FIG. 3. (Color online) Decay curve of $^{210}$Po in the slice metal sample over about 350 d.

of samples. Each type has one sample. Finally, the $\alpha$ decay half-life of $^{210}$Po was measured in both types of samples. Figures 1 and 2 are typical $\alpha$ spectra of $^{210}$Po in the Bi film and the Bi slice, respectively, at room temperature.

The LISE++ software was used to calculate the $\alpha$ particle straggling and energy loss in bismuth metal. The alpha particles will be fully stopped after 16.9 $\mu$m, which is thus the maximum depth to observe $\alpha$ decay from the metallic sample.

In addition, if there is a lattice defect, it may lead to large errors when measuring the alpha half-life, because radionuclides may diffuse in the sample. If $^{210}$Po diffuses in Bi, changes in the measured half-life may be mistaken for electronic shielding effects. After annealing, $^{210}$Po content (with a fraction of $10^{-8}$) was firmly fixed in the Bi lattice.

Controlling the systematic error is very important. If the systematic error is too large, a difference in the measured half-life might be mistaken and falsely attributed to the electronic shielding effect. The dead time was determined to be less than 0.50%. Uncertainty in the geometry is less than 0.20%. During the data acquisition, we simultaneously added a fixed signal from a research pulser to monitor any artificial drift in the peak position.

The samples were coupled to the detector coaxially through a socket-shaped bracket which was made of polytetrafluoroethylene. The effective detection area was limited by the effective diameter of the $\alpha$ detector and the solid angle was fixed in each measurement.

The half-life of $^{210}$Po is given by Eq. (1), where the decay constant $\lambda$ is obtained using Eq. (2), with $N_0$ and $N_t$ standing for $\alpha$ counting rates at decay time of 0 and $t$, respectively:

$$T_{\frac{1}{2}} = \ln 2/\lambda, \tag{1}$$

$$N_t = N_0 e^{-\lambda t}. \tag{2}$$

The results are represented in Figs. 3 and 4 and are initially fit with solid curves. To determine the best fit to the data, we used a regression analysis on the data. Simulations showed that the best fit converged well. We then repeated the linear regression for a straight line. We used a reduced $\chi^2$ analysis—$\chi^2/\nu$, where $\nu = n - 2$ is the number of degrees of freedom

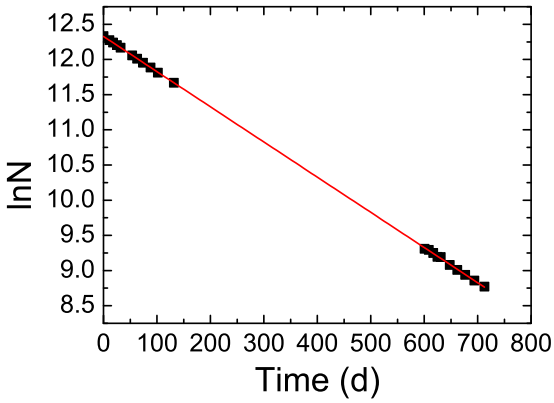


FIG. 4. (Color online) Decay curve of $^{210}$Po in the film metal sample over about 700 d.

and $n$ is the number of data points. From our fits, we obtained a value close to one for the reduced $\chi^2$, representing a good fit to the data. The uncertainties we determine are $1\sigma$ from the best fit (using $\chi^2_{\min}+1$) [26]. Summaries of the uncertainties for the film and slice samples are presented in Tables I and II, respectively. We determine a half-life for $^{210}$Po of $138.87\pm 0.87$ d ($\chi^2/\nu=1.69$) in the slice sample, measured over the course of 350 d. These data and the corresponding decay curve are shown in Fig. 3. We also find a half-life of $138.40\pm 0.21$ d ($\chi^2/\nu=1.17$) for $^{210}$Po in the metal film sample, which we measured for 700 d. These data and decay curve are shown in Fig. 4. Both of our measurements are consistent with the accepted value of 138.3763(17) d for the half-life of $^{210}$Po [24].

## IV. DISCUSSION

Figures 1 and 2 show the $\alpha$ spectra of the slice and film samples, respectively, over a range of 3.00–5.30 MeV, which was the region of interest for the measurement of the rate of $\alpha$ decay in our samples. In the slice sample, $^{210}$Po atoms were distributed homogeneously in a $^{209}$Bi matrix after irradiation and annealing. The $\alpha$ particles show some energy loss, indicating that they originated from $^{210}$Po nuclides imbedded deeply in the slice sample. Note that the electron density of the film sample ($^{210}$Po @$Bi_2O_3$) is lower than that in the slice sample ($^{210}$Po @Bi metal) by about nine orders of magnitude. It is also worthwhile to mention that there is no evidence of $^{210}$Po diffusion to the surface of either sample in this experiment.

TABLE I. Uncertainty contributions of the half-life of the $^{210}$Po film.

| Components | $\Delta T_{1/2}/T_{1/2}$(%) |
|---|---|
| Statistical uncertainty | 0.11 |
| $\alpha$ energy-range | 0.20 |
| Geometric influence | 0.10 |
| Total | 0.15 |

TABLE II. Uncertainty contributions of the half-life of the $^{210}$Po slice.

| Components | $\Delta T_{1/2}/T_{1/2}$(%) |
|---|---|
| Statistical uncertainty | 0.59 |
| $\alpha$ energy-range | 0.20 |
| Geometric influence | 0.10 |
| Total | 0.63 |

Alpha particles have to tunnel the Coulomb barrier in the opposite direction compared to low-energy nuclear reactions. The tunneling probability is related to the so-called penetration factor. The decay constant of $\alpha$ decay is proportional to this penetration factor. Thus it is possible that the decay constant could be modified by a cloud of quasifree metallic electrons around the atomic nucleus [27]. Indeed, previous calculations have indicated that the metallic electron screening effect was small [14,19] and there has even been some improvement in the theory [14]. However, Zinner [23] showed that the electron screening reduces not only the Coulomb barrier among interacting nuclei but also influences the repulsion Coulomb potential inside the nucleus. That is to say that electron screening should affect not only the Coulomb barrier, but also the $\alpha$ energy inside the nucleus.

However, if the internal and external screening energies have the same values, the penetration coefficient and the decay constant do not change at all. A recent study demonstrated that the electron screening potential in the inner part of a nucleus is smaller than in the external region due to the energy of the $\alpha$ particle; this difference should lead to a slightly increased $\alpha$ decay rate in a metallic environment [13]. Eliezer *et al.* [28] calculated a decrease of about 1% of the decay half-life for $^{210}$Po embedded in Pd at $T=4$ K. However, from Ref. [3], the temperature effect was negligible. In Fig. 5, we show a comparison between the two values we determined for the half-life of $^{210}$Po in this study and the accepted reference value [24,25]. Here, we see that the half-lives we determine are slightly longer than the reference value of 138.3763(17) [24,25], but all three values agree within their error bars. Thus,

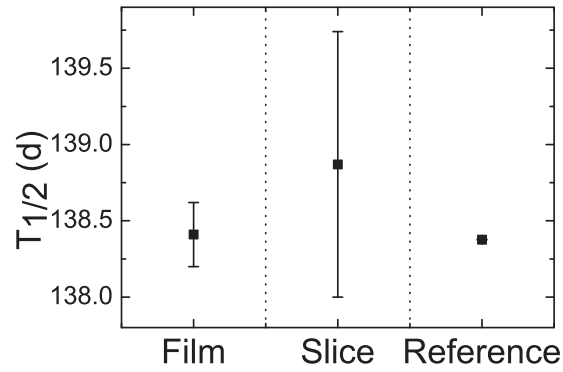


FIG. 5. Plot of the two determined half-lives along with the reference value (error bars represent $1\sigma$). All two half-lives are longer than the one given in the reference.

we could not detect any significant change between the half-life of $^{210}$Po in a thin film or a metallic slice.

## V. CONCLUSION

We successfully created a film sample ( $^{210}$Po @$Bi_2O_3$) and a slice sample ($^{210}$Po @Bi metal). Using the film sample as a reference, we measured the half-life of $^{210}$Po in each sample and determined that they were slightly longer than the accepted reference value but within their uncertainties they are consistent with the literature value, meaning that there is effectively no difference between them.

The half-lives we determined experimentally are also within the uncertainties of the results predicted by the Debye plasma model in a film sample and a slice sample. The Debye plasma model might therefore not be taking into account certain physical factors which can be found in the literature [23], or it may be that the large uncertainties on our data prohibited us from detecting such a small change.

While we sought to examine the effect of the local environment on the half-life of $^{210}$Po by directly measuring the half-life in both a film and metal slice sample at room temperature, we were unable to observe any statistically significant difference between the two. Due to the limited precision in this study, we are not sensitive to changes in the half-life that are less than 0.63%. Thus, this issue still remains unresolved.

However, our experiment provides and independent examination of the existing data and a basis for further experiments. A future improved experiment could be, e.g., to use cryogenic temperatures, a strong electric field, and a strong magnetic field to study the relationship between the effect of screening by quasifree electrons and the half-lives of radionuclides.

## ACKNOWLEDGMENTS

The authors wish to acknowledge the support of the Dr. D. Kahl (University of Tokyo), Dr. S. E. Malek, Dr. S. T. Wang, Professors S. H. Zhou, Z. H. Li, C. J. Lin, J. Su, S. Q. Yan, B. Guo, Y. J. Li, H. L. Ma, H. M. Jia, and C. B. Li for helpful discussion and suggestions. This study was funded by the National Natural Science Foundation of China under Grant Nos. 10875177, 11175263, 11265005, 11375272, and 11565008.

[1] T. Ohtsuki *et al.*, Phys. Rev. Lett. **93**, 112501 (2004).
[2] T. Ohtsuki *et al.*, Phys. Rev. Lett. **98**, 252501 (2007).
[3] P. Poml *et al.*, Phys. Rev. C **89**, 024320 (2014).
[4] A. Y. Dzyublik, Phys. Rev. C **90**, 054619 (2014).
[5] J. Su, Eur. Phys. J. A **46**, 69 (2010).
[6] F. Raiola *et al.*, Eur. Phys. J. A **32**, 51 (2007).
[7] B. Wang *et al.*, Eur. Phys. J. A **28**, 375 (2006).
[8] F. Wauters *et al.*, Phys. Rev. C **82**, 064317 (2010).
[9] N. Severijns *et al.*, Phys. Rev. C **76**, 024304 (2007).
[10] Y. Nir-El *et al.*, Phys. Rev. C **75**, 012801(R) (2007).
[11] Z. Patyk *et al.*, Phys. Rev. C **78**, 054317 (2008).
[12] H. B. Jeppesen, Eur. Phys. J. A **32**, 31 (2007).
[13] K. Czerski *et al.*, Acta Phys. Pol. B **40**, 903 (2009).
[14] K. Kettner *et al.*, J. Phys. G: Nucl. Part. Phys. **32**, 489 (2006).
[15] S. H. Zhou, Chin. Phys. C **35**, 449 (2011).
[16] K.-J. Dong *et al.*, Chin. Phys. Lett. **29**, 072301 (2012).
[17] S. Pierre, Appl. Radiat. Isot. **68**, 1467 (2010).
[18] H. Muir, New Sci. **2574**, 36 (2006).
[19] G. T. Emery, Annu. Rev. Nucl. Sci. **22**, 165 (1972).
[20] M. S. Freedman, Annu. Rev. Nucl. Sci. **24**, 209 (1974).
[21] H. P. Hahn, Radiochim. Acta **23**, 23 (1976).
[22] F. Raiola *et al.*, J. Phys. G: Nucl. Part. Phys. **31**, 1141 (2005).
[23] N. T. Zinner, Nucl. Phys. A **781**, 81 (2007).
[24] J. F. Eichelberger, Technical Report, United States Atomic Energy Commission, 1964, Mound Laboratory Report for July 1964 .
[25] F. G. Kondev, Nucl. Data Sheets **109**, 1527 (2008).
[26] P. McCullagh and J. A. Nelder, *Generalized Linear Models*, 2nd ed. (Chapman and Hall/CRC, Boca Raton, FL, 1989).
[27] E. E. Salpeter, Aust. J. Phys. **7**, 373 (1954).
[28] S. Eliezer, Phys. Lett. B **672**, 372 (2009).